# Experimental application of individual column state and parameter estimation in SMB processes to an amino acid separation

**Stefanie Gerlich** [*] **Hind Arab** [*] **Malte Buchholz** [*]
**Sebastian Engell** [*]

[*] *Process Dynamics and Operations Group, TU Dortmund University,*
*Emil-Figge-Str. 70, 44227 Dortmund, Germany (e-mail:*
*stefanie.gerlich@tu-dortmund.de).*

Abstract    The simulated moving bed (SMB) process is a highly efficient continuous chromatographic separation process. Due to its hybrid process dynamics that lead to discontinuities and sharp fronts on the state trajectories, optimal SMB process operation is challenging. Process performance can be improved by applying model-based optimizing control methods. For this, online information about states and individual column parameters are required. The strategy for simultaneous state and parameter estimation used here exploits the switching nature of the SMB process. The successful experimental application of the strategy is demonstrated for the continuous separation of two amino acids on an SMB pilot plant where extra-column equipment effects need to be considered.

*Keywords:* State estimation, parameter estimation, chromatography, simulated moving bed process, experimental application

## 1. INTRODUCTION

Chromatography is gaining importance as a separation technique as the production of fine chemicals, pharmaceuticals and biotechnological products increases. For these products, that are produced at small scale, chromatography is the method of choice for separation due to its high selectivity, comparatively low operating temperatures and handling of aqueous solutions (Guiochon et al., 2006). Usually, these chromatographic separations are performed in batch mode. In this operation mode however, the stationary phase is poorly used and large amounts of desorbent (mobile phase) are consumed leading to low product concentrations.

In order to improve the separation efficiency and to use the stationary phase more efficiently, the continuously operated simulated moving bed (SMB) process can be used for the separation of binary mixtures (Rajendran et al., 2009). This multicolumn chromatographic process simulates a countercurrent flow of the stationary and mobile phase by periodically switching the inlet and outlet ports between the individual columns (Schmidt-Traub et al., 2020). Figure 1 shows the widely used 4-zone SMB process with 2 columns per zone. The inlet (desorbent and feed) and outlet (extract and raffinate) ports define the location of 4 characteristic zones. The stronger retained component (B) is collected at the extract, while the less retained component (A) is received at the raffinate.

The periodic switching of the ports in the SMB process leads to a cyclic steady state (CSS) at which the concentration profile at the outlet ports is repeated from period to period. Due to these hybrid dynamics that lead to discon-
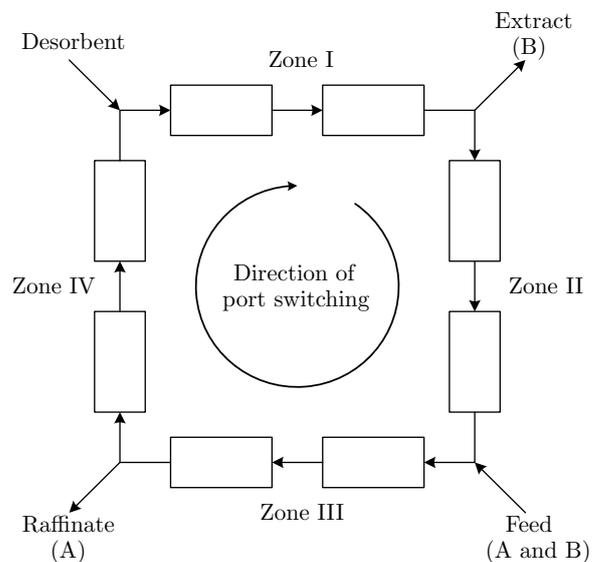


Figure 1. Schematic representation of a 4-zone SMB process with 2 columns per zone.

tinuities and sharp fronts in the state trajectories, optimal operation of the SMB process is challenging. The efficiency of SMB processes can be improved using model-based optimizing control techniques such as linear or nonlinear model predictive control ((N)MPC) that are based on a detailed process model considering the hybrid dynamics of the SMB process directly (Engell, 2007). The use of such methods requires online information about states and parameters of the system.

In the pioneering work of Toumi and Engell (2004), the states of the SMB process were obtained by forward simulation of a plant model. In Küpper et al. (2009) a moving horizon state and parameter estimation scheme for SMB processes was proposed. Both approaches assume uniform properties of all columns in the SMB system which is not realistic in practice as the columns are not identically packed with adsorbent. Thus, individual column parameter estimation can improve process operation and can help to detect degrading columns during process operation.

The challenge regarding individual column parameter estimation in SMB processes is that only scarce measurement information is available. An extended-Kalman-filter-based method for estimating individual column parameters using concentrations measurements at the two outlet ports and at one fixed location between the columns has been presented by Küpper and Engell (2006). Lemoine-Nava and Engell (2014) developed an optimization-based scheme for estimating the parameters of each column individually from concentration measurements in the extract and raffinate streams only. In Gerlich et al. (2020) this scheme was applied to the continuous separation of two amino acids in a simulation study. It was shown that the estimation scheme can be used already during process start-up and is capable of dealing with plant-model mismatch in the column porosities.

When applying online process monitoring schemes to experimental SMB processes, the influence of extra-column equipment such as pumps, pipes, valves and detectors needs to be considered as it causes back-mixing and delay. Approaches in the literature for handling extra-column equipment effects include the extension of the ideal SMB model by standard mass balance models for plug flows and CSTs (Lee et al., 2020) or summarizing all extra-column dead volumes in each zone (Grossmann et al., 2010).

In this contribution, estimating individual column parameters and handling extra-colum equipment effects simultaneously is addressed. The state and parameter estimation concept introduced by Lemoine-Nava and Engell (2014) is applied to a small-scale SMB process performed on commercial equipment for the continuous separation of two amino acids, methionine and phenylalanine. Concentrations measurements are only available at the extract and raffinate ports. We show that it is sufficient to lump all extra-column equipment effects into one plug flow reactor model at each outlet and that individual column parameters can be estimated successfully.

The remainder of the paper is structured as follows. First, the used first principle model is explained. Second, the state and parameter estimation scheme is introduced and the handling of extra-column equipment effects is discussed. Afterwards, the scheme is applied to the continuous separation of two amino acids, methionine and phenylalanine, on a pilot plant SMB process. The paper is concluded with a discussion of the outcomes and future prospects are outlined.

## 2. MODELING OF THE SMB PROCESS

Approaches to modeling SMB processes either assume a true counter-current flow of the mobile and stationary phase, or they directly consider the switching dynamics of the SMB process. The latter is employed in this paper to achieve a higher accuracy of the model.

In order to consider its switching dynamics, the SMB process is modeled via the interconnection of models for each individual column via node balances:

$$0 = -Q_I + Q_{IV} + Q_{Des} \tag{1}$$
$$0 = -Q_{II} + Q_I - Q_{Ex} \tag{2}$$
$$0 = -Q_{III} + Q_{II} + Q_{Fe} \tag{3}$$
$$0 = -Q_{IV} + Q_{III} - Q_{Raf} \tag{4}$$
$$0 = -c_{j,in,I}Q_I + c_{j,out,IV}Q_{IV} \tag{5}$$
$$0 = -c_{j,in,III}Q_{III} + c_{j,out,II}Q_{II} + c_{j,Fe}Q_{Fe}, \tag{6}$$

where $Q_a$ represents the flow rate in the respective zone or at the respective port. $c_j$ refers to the concentration of component $j$.

The dynamic modeling of the individual column behavior is widely studied in literature. An overview of different models can be found in Schmidt-Traub et al. (2020). In this contribution, the transport dispersive model (TDM) is chosen (Guiochon et al., 2006; Schmidt-Traub et al., 2020) because of its simplicity and sufficient accuracy for solutes with low molecular weights (Schmidt-Traub et al., 2020) such as amino acids.

For each individual column, the dynamic mass balance equations along the column length coordinate $z$ for each component in the liquid phase is given as:

$$\frac{\partial c_j}{\partial t} + u_{int}\frac{\partial c_j}{\partial z} + \frac{1-\epsilon_b}{\epsilon_b}k_{eff,j}\frac{3}{r_p}(c_j - c_{p,j}) = D_{ax}\frac{\partial^2 c_j}{\partial z^2} \tag{7}$$

where $c_j$ and $c_{p,j}$ represent the liquid and particle phase concentrations of component $j$. The radius of the porous particles is represented by $r_p$. $k_{eff,j}$ is the lumped film transfer coefficient of component $j$, and the axial dispersion coefficient is denoted by $D_{ax}$. The interstitial fluid velocity $u_{int}$ depends on the volumetric flow rate $Q$ in the respective column, on the cross-sectional area of the column $A_c$, and the column void fraction $\epsilon_b$:

$$u_{int} = \frac{Q}{A_c\epsilon_b} \tag{8}$$

Here, the axial dispersion coefficient $D_{ax}$ is calculated based on the empirical correlation by Chung and Wen (1968):

$$\text{Pe}_p = \frac{0.2}{\epsilon_b} + \frac{0.011}{\epsilon_b}\left[\text{Re}_p\epsilon_b\right]^{0.48} \tag{9}$$

where $\text{Pe}_p$ and $\text{Re}_p$ are the particle Péclet number and the particle Reynolds number,

$$\text{Pe}_p = \frac{2u_{int}r_p}{D_{ax}}, \quad \text{Re}_p = \frac{2u_{int}r_p\rho}{\eta}, \tag{10}$$

and $\rho$ and $\eta$ are the liquid phase density and dynamic viscosity. The mass balance equation of component $i$ in the particle phase for each individual column is given as:

$$\epsilon_p\frac{\partial c_{p,j}}{\partial t} + (1-\epsilon_p)\frac{\partial q_j}{\partial t} = k_{eff,j}\frac{3}{r_p}(c_j - c_{p,j}), \tag{11}$$

where $q_j$ refers to the concentration of component $j$ in the adsorbed phase and $\epsilon_p$ describes the particle porosity. The adsorption equilibrium between the concentration of the adsorbed component and the concentration in the particle phase is described by the Langmuir isotherm (Schmidt-Traub et al., 2020):

$$q_j = \frac{H_j c_{p,j}}{1 + \sum_{n=1}^{N_{comp}} b_i c_{p,i}} \quad (12)$$

$H_j$ and $b_i$ are the Langmuir isotherm parameters of components $j$ and $i$. The number of components is represented by $N_{comp}$. For a binary system with components A and B where A is the less retained component and B is the stronger retained component, $H_B > H_A$. The set of PDEs is completed with the following initial and boundary conditions:

$$\text{at } t = 0: \quad c_j(0, z) = c_{j,0}, \quad c_{p,j}(0, z) = c_{p,j,0} \quad (13)$$

$$\text{at } z = 0: \quad u_{int} c_j - D_{ax} \frac{\partial c_j}{\partial z}\Big|_{z=0} = u_{int} c_{j,in} \quad (14)$$

$$\text{at } z = L_c: \quad \frac{\partial c_j}{\partial z}\Big|_{z=L_c} = 0, \quad (15)$$

where $L_c$ represents the column length.

The PDEs required for column modeling (equations (7) and (11)) are spatially discretized using a finite volume approach combined with the weighted essentially non-oscillatory (WENO) scheme (von Lieres and Andersson, 2010). The method is suitable for handling systems with sharp concentration fronts which appear in chromatographic columns.

## 3. STATE AND PARAMETER ESTIMATION IN SMB PROCESSES

A scheme for online process monitoring in SMB processes that estimates states and individual column parameters has been proposed by Lemoine-Nava and Engell (2014). The scheme exploits the switching nature of the SMB process that results in a movement of the measurement locations in each period.

For estimating the process states, the process model described in section 2 is simulated with the current inputs and the current parameter estimates from the parameter estimation routine. Inlet concentrations that are fed to the columns behind the measurement locations are the measured concentrations at the extract and raffinate ports.

The main idea regarding the parameter estimation routine is to represent the process by two virtual batch experiments for each column during each cycle of the SMB process when the respective column is situated before and after the extract and raffinate ports as illustrated in figure 2. During a period $k$, measurements are first collected at the inlet of column $i$ and in the next period $k + 1$, the concentrations are measured at the outlet of the respective column. Thus, each virtual batch experiment has a length of two periods. For estimating the parameters of each column, the following least-squares optimization problem is solved periodically that seeks to minimize the deviations between measured and simulated concentrations:

$$\min_{\substack{\hat{\underline{p}}_i^{k+1}, \hat{\underline{x}}_i(T^{k-1}), \\ \hat{\underline{x}}_i(T^{k-\Pi-1})}} \quad \frac{1}{\sigma_p} \left\| \hat{\underline{p}}_i^{k-N_{col}+1} - \hat{\underline{p}}_i^{k+1} \right\|^2 \quad (16)$$

$$\frac{1}{\sigma_x} \left\| \begin{matrix} \hat{\underline{x}}_i(T^{k-N_{col}-1}) - \hat{\underline{x}}_i(T^{k-1}) \\ \hat{\underline{x}}_i(T^{k-\Pi-N_{col}-1}) - \hat{\underline{x}}_i(T^{k-\Pi-1}) \end{matrix} \right\|^2$$

$$\frac{1}{\sigma_m} \left\| \begin{matrix} \underline{y}_i^{k+1,j}(t) - \hat{\underline{y}}_i^{k+1,j}(t) \\ \underline{y}_i^{k-\Pi+1,j}(t) - \hat{\underline{y}}_i^{k-\Pi+1,j}(t) \end{matrix} \right\|^2$$
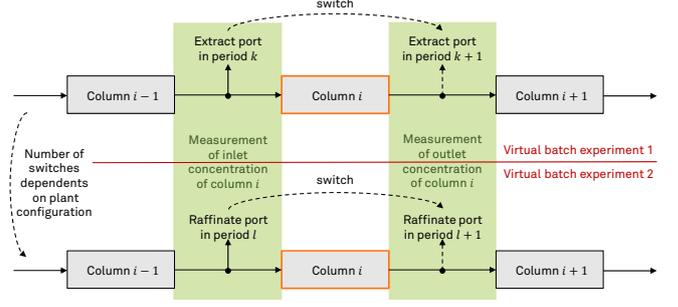


Figure 2. Scheme for individual column parameter estimation in SMB processes

$$\text{s.t.} \quad \hat{\underline{x}}_i(T^{\gamma+1}) = \hat{\underline{x}}_i(T^{\gamma-1})$$

$$+ \int_{T^{\gamma-1}}^{T^{\gamma}} f\left(\hat{\underline{x}}_i(t), \underline{u}_i^{\gamma-1}(t), \hat{\underline{p}}_i^{k+1}\right) dt$$

$$+ \int_{T^{\gamma}}^{T^{\gamma+1}} f\left(\hat{\underline{x}}_i(t), \underline{u}_i^{\gamma}(t), \hat{p}_i^{k+1}\right) dt, \quad (17)$$

$$\hat{\underline{x}}_i = \left[\hat{\underline{C}}_i^{b,j}, \hat{\underline{C}}_i^{p,j}\right]^T, \quad j = \{A, B\}, \quad (18)$$

$$\underline{u}_i^{\gamma-1}(t) = \left[Q_i^{\gamma-1}, \tau, \underline{y}_{i-1}^{\gamma-1}(t)\right]^T, \quad (19)$$

$$\underline{u}_i^{\gamma}(t) = \left[Q_i^{\gamma}, \tau, \underline{\hat{C}}_{out,i-1}^{\gamma}(t)\right]^T, \quad (20)$$

$$\hat{\underline{x}}_i^l \le \hat{\underline{x}}_i \le \hat{\underline{x}}_i^u, \quad (21)$$

$$\hat{\underline{p}}_i^l \le \hat{\underline{p}}_i \le \hat{\underline{p}}_i^u, \quad (22)$$

$$\gamma = \{k - \Pi, k\}, \quad (23)$$

$$\Pi = N_{col,I} + N_{col,IV}, \quad (24)$$

$$\hat{\underline{y}} = x_{N_z} \quad (25)$$

with the index $k$ for period, the vector of estimated states parameters of column $i$ as $\hat{\underline{x}}_i$ and $\hat{\underline{p}}_i$, the input vector of column $i$ as $\underline{u}_i$, the simulated outlet concentrations of component $j$ and column $i$ as $\hat{\underline{y}}_i^j$ and measured outlet concentrations of component $j$ and column $i$ as $\underline{y}_i^j$. $\Pi$ is the sum of the number of columns in zones I and IV.

During one full cycle of the SMB process, the parameters of each column are updated once using data from four sets of measurements which are obtained when the extract and the raffinate port are at the inlet and outlet of the column respectively. The parameter estimation is activated as soon as enough measurement information is available for the first column, in the case considered here after the sixth port switching. Details regarding the implementation of the scheme are given in Gerlich et al. (2020).

## 4. HANDLING OF EXTRA-COLUMN EQUIPMENT

In real SMB processes, the influence of extra-column equipment such as pumps, valves, pipes, and detectors cannot be neglected, especially for small scale plants. Pumps and pipes connecting the different parts of the equipment cause delay when molecules travel through the plant. Back-mixing effects are introduced by measuring cells within the detectors. Here, the volume of the measuring cells in the detectors is only $2\,\mu\text{L}$ and thus, it can be neglected.

SMB experiments at the pilot plant revealed that the delay that is observed between the switching of the valves and

the resulting jump in the concentration profile is the same from period to period, independent of the of the current connection of valves, pumps, and columns. Therefore, it is sufficient to summarize all delays due to extra-column equipment in one plug flow reactor at each outlet stream before the detectors as shown in figure 3. The observed delay is approximately 20% of the duration of one period although the ratio between all dead volumes in the plant and the volume of all columns is only 5%.
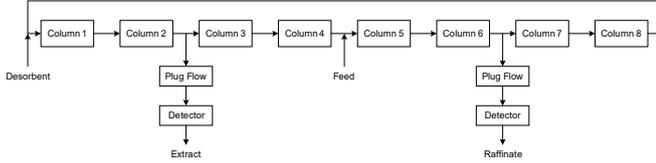


Figure 3. Modeling of extra-column equipment

This approach has several advantages over other described strategies in the literature. First, it is much simpler. Furthermore, the SMB process model that is used for state and parameter estimation as well as for model-based optimization does not need to be adapted for extra-column equipment effects. The plant measurements that are used for state and parameter estimation are those that occur directly at the column outlet before the plug flow element (see figure 3). This might not be the true concentration at this location at a certain point in time but results in a consistent model.

## 5. CASE STUDY: CONTINUOUS SEPARATION OF AMINO ACIDS USING THE SMB PROCESS

The continuous separation of two amino acids, methionine and phenylalanine, using a 4-zone SMB process with two columns per zone is studied in this contribution. The desorbent consists if of de-ionized water and 5 vol% methanol in addition to the buffer potassium dihydrogen phosphate with a concentration of 0.1 M. The pH is regulated to 3 by adding orthophosphoric acid. Component and solvent specific parameters are given in tables 1 and 2. As $H_{Met} < H_{Phe}$ (see table 1), phenylalanine represents the stronger adsorbing component and is retrieved at the extract port while methionine is collected at the raffinate port.

Table 1. Initial model parameters
(Met = methionine, Phe = phenylalanine)

|  | Met | Phe |
| --- | --- | --- |
| $H_{i,initial}$ [-] | 1.3133 | 10.9281 |
| $b_i$ [L/g] | 0.008 | 0.002 |
| $k_{eff,i}$ [m/s] | $8.03 \cdot 10^{-6}$ | $1.01 \cdot 10^{-4}$ |

The parameters $H_{Met}$ and $H_{Phe}$ are estimated by the online process monitoring scheme introduced in section 3 as a simulation study revealed that various effects resulting from an offset in a different parameter can be lumped into the isotherm parameter $H_i$ (Gerlich et al., 2020). The initial estimates for $H_i$ as well as the parameter values for the isotherm parameter $b_i$, the mass transfer coefficient and column porosities were determined in batch experiments on a single column of the system in which either a sample of methionine and phenylalanine or a tracer were injected.

Table 2. Column and solvent parameters

| Parameter | Description | Value |
| --- | --- | --- |
| $L_c$ | column length | 0.125 m |
| $A_c$ | column cross sectional area | $5.03 \cdot 10^{-5}$ m$^2$ |
| $r_p$ | particle diameter | $15 \cdot 10^{-6}$ m |
| $\epsilon_b$ | void fraction | 0.80 |
| $\epsilon_p$ | particle porosity | 0.26 |
| $\rho$ | eluent density | 1000 kg/m$^3$ |
| $\eta$ | dynamic viscosity | $10^{-3}$ Pas |

### 5.1 SMB equipment

The separation is realized on an SMB pilot plant with eight columns that is manufactured by KNAUER Wissenschaftliche Geräte GmbH. The chromatography columns used are based on silica gel containing nonpolar and monomeric octadecyl. Thus, reversed-phase chromatography is used, where the stationary phase is nonpolar and the mobile phase is polar. The column and solvent specific parameters are summarized in table 2. Multiposition valves are used to set up the connections corresponding to each period. Multiwavelength UV-detectors that are able to measure the absorbance at up to four different wavelengths simultaneously are placed at the extract and raffinate ports. For the case study in this contribution, absorbance is measured at 200, 210, 220 and 225 nm.

### 5.2 Absorption measurements and data reconciliation

The absorption measured by the multi-wavelength UV-detectors at a certain wavelength is related to the composition in a nonlinear fashion:
$$y = f(c_M, c_P), \tag{26}$$
where $y \in \mathbb{R}^{4 \times 1}$ represents the four measured absorptions at four different wavelengths. $c_M$ and $c_P$ are the concentration of methionine and phenylalanine. The correlation between the measured absorption at a given wavelength $k$ and the concentration has the following form:
$$y_k = a_{1,k}c_M + a_{2,k}c_P^2 + a_{3,k}c_P + a_{4,k}c_M c_P \tag{27}$$
The coefficients $a_{j,k}$ were determined from calibration experiments. As four measurements are available, but only two concentrations need to be retrieved from that, there are more measurements available than needed. Thus, the following least squares optimization problem is solved for every sampling point for both outlet streams to obtain the estimate of the true concentrations:
$$\min_{c_M, c_P} \sum_{k=1}^{4} (y_{k,meas} - y_{k,calc})^2 \tag{28}$$
$$\text{s.t} \quad y_{k,calc} = f(c_M, c_P). \tag{29}$$

## 6. RESULTS AND DISCUSSION

In this section, experimental results and the performance of the state and parameter estimation scheme are discussed.

### 6.1 SMB process operation

In practical applications, the operating conditions of SMB processes are usually determined using the triangle theory

(Mazzotti et al., 1997) and are applied to the process via feedforward control. The triangle theory represents a shortcut design method for SMB processes. Due to the assumption of a true countercurrent flow between the mobile phase and the stationary phase, the resulting operating conditions are suboptimal for the real SMB process. Off-spec production can result for SMB processes with few columns where the deviations to a true countercurrent flow increase (Erdem et al., 2004).

Here, the operating conditions were determined based on the triangle theory with the initial estimates of the isotherm parameter $H_i$ as given in table 1. The feed contains $0.2$ g/L of methionine and phenylalanine and the ports are shifted every two minutes giving a period length of $\tau = 2$ min. The process is operated with $Q_I = 8.10$ mL/min, $Q_{Des} = 5.02$ mL/min, $Q_{Ex} = 3.55$ mL/min, and $Q_{Fe} = 2.36$ mL/min. The resulting plant measurements are shown in figure 4.
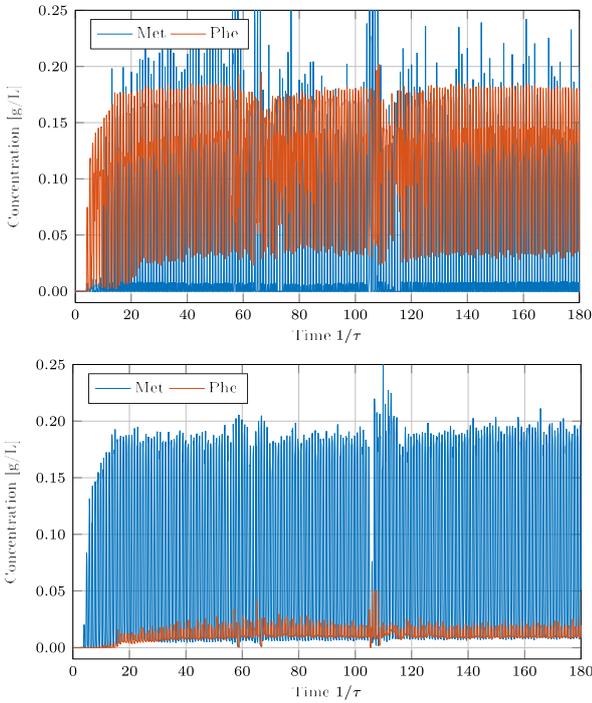


Figure 4. Concentration measurements at extracte (top) and raffinate (bottom) for an SMB experiment over 180 periods.

Phenylalanine is the dominant component at the extract port while the less adsorbing component methionine is retrieved at the raffinate port. Both products, the extract and raffinate, are contaminated while from the triangle theory pure products would be expected. This observation emphasizes that often only suboptimal operating points or operating points that do not fulfill process constraints are achieved when applying the triangle theory to a real SMB process. Further observations from figure 4 are that a cyclic steady state is reached after about 20 periods. The profiles indicate slight variations between the columns. Thus, it is important to estimate each parameters of each column individually. Also, disturbances occur during process operations such as around period 60 and period 100.

## 6.2 Performance of the state and parameter estimation scheme

The performance of the estimation scheme for the states and parameters of the indivdual columns introduced in section 3 is analyzed for the experimental data. The development of the values of the estimated parameters over 180 periods of operation is presented in figure 5.
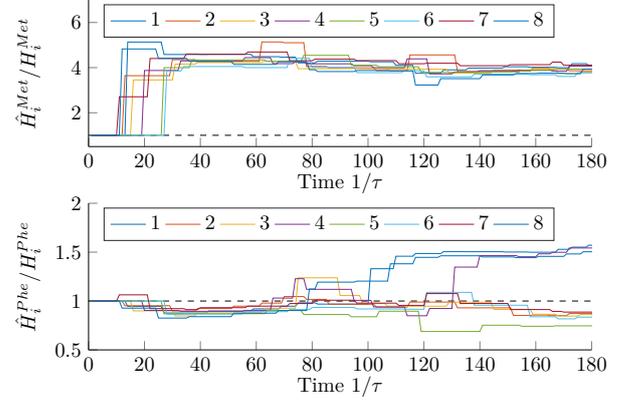


Figure 5. Convergence of estimated parameters $H_{Met}$ (top) and $H_{Phe}$ (bottom) over 180 periods of operation

It can be seen that the changes of the parameter $H_{Met}$ are much larger compared to those for the parameter $H_{Phe}$. The online process monitoring scheme is capable of dealing with such large plant-model mismatches. Thus, the preliminary experimental effort for determining model parameters can be reduced significantly. It is sufficient to perform preliminary batch-experiments on a single column of the SMB system and assume identical parameters for all columns initially. Afterwards, model parameters can be adapted for each column individually during SMB process operation. The parameters for all columns converge to a constant value at around period 40 and show only slight variations between periods 40 and 60. These variations are caused by measurement noise.

When an unmodeled disturbance occurs in the measured data, this is captured in the parameter estimation by adapting the column parameters. For the parameter related to methionine, $H_{Met}$, it can be seen that the parameter values converge back to the value before the disturbance. In contrast, the values for the parameter related to phenylalanine, $H_{Phe}$, converge to a different value indicating a changing behavior of the columns regarding the adsorption of phenylalanine.

In figure 6, measured and estimated states at the extract and raffinate ports are compared as plant measurements are available at that position. It can be observed that the deviations between the measured and the estimated states are initially quite large for methionine reflecting again, that the initial estimate of the methionine isotherm parameter $H_{Met}$ is not quite inaccurate.

Once the parameters have converged to a constant value, the concentration profiles at the extract and raffinate ports can be predicted well by the state estimation. Thus, besides being useful for the adaptation of the initial guesses of the process parameters and process monitoring, the
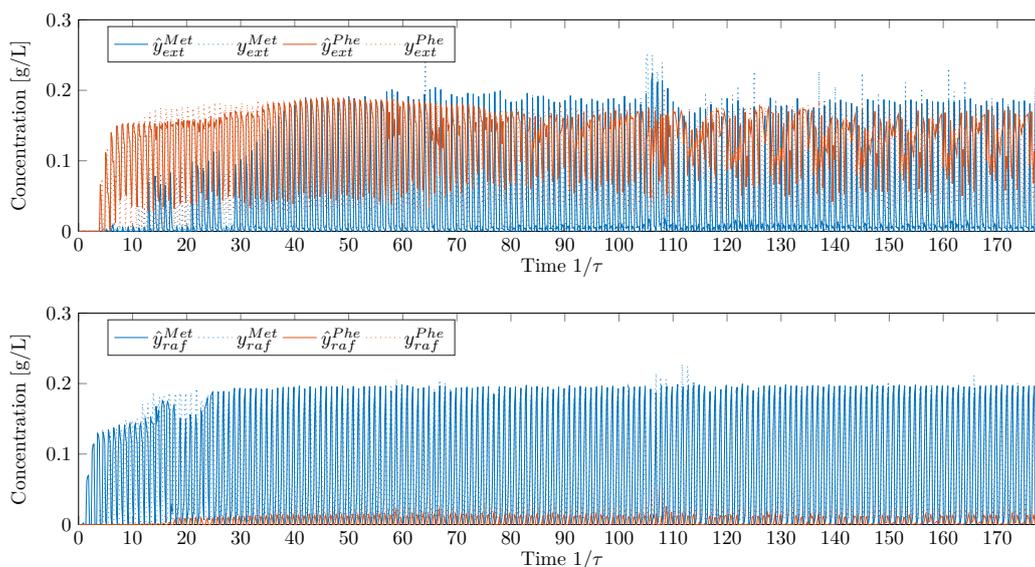
Figure 6. Comparison of measured and estimated states at extract (top) and raffinate (bottom) over 180 periods of operation

scheme can be used for model-based optimizing control to improve the performance of the process.

## 7. CONCLUSION AND FUTURE WORK

In this work, an online process monitoring scheme including the estimation of individual columns parameters that has been successfully tested in simulation studies by Gerlich et al. (2020) is successfully applied to an experimental pilot plant SMB process. For many SMB processes, extra-column equipment effects cannot be ignored. It has been shown that it is sufficient to lump all time delays caused by extra-column dead volumes in one plug flow element at each outlet. With this extension, the scheme can handle large plant-model mismatches. The scheme will be combined with model-based optimizing control to ensure fast start-up and optimal SMB process operation also in the case where the columns do not behave identically.

## REFERENCES

Chung, S.F. and Wen, C.Y. (1968). Longitudinal dispersion of liquid flowing through fixed and fluidized beds. *AIChE Journal*, 14(6), 857–866.

Engell, S. (2007). Feedback control for optimal process operation. *Journal of Process Control*, 17(3), 203–219.

Erdem, G., Abel, S., Morari, M., Mazzotti, M., Morbidelli, M., and Lee, J.H. (2004). Automatic Control of Simulated Moving Beds. *Industrial and Engineering Chemistry Research*, 43(2), 405–421.

Gerlich, S., Misz, Y.N., and Engell, S. (2020). Online Process Monitoring in SMB Processes. *Computer Aided Chemical Engineering*, 48, 1261–1266.

Grossmann, C., Langel, C., Mazzotti, M., Morari, M., and Morbidelli, M. (2010). Experimental implementation of automatic 'cycle to cycle' control to a nonlinear chiral simulated moving bed separation. *Journal of Chromatography A*, 1217(13), 2013–2021.

Guiochon, G., Shirazi, D.G., Felinger, A., and Katti, A.M. (2006). *Fundamentals of preparative and nonlinear chromatography*. Academic Press.

Küpper, A., Diehl, M., Schlöder, J.P., Bock, H.G., and Engell, S. (2009). Efficient moving horizon state and parameter estimation for SMB processes. *Journal of Process Control*, 19(5), 785–802.

Küpper, A. and Engell, S. (2006). Parameter and state estimation in chromatographic SMB processes with individual columns and nonlinear adsorption isotherms. *IFAC Proceedings Volumes*, 39(2), 611–616.

Lee, J.W., Kienle, A., and Seidel-Morgenstern, A. (2020). On-line optimization of four-zone simulated moving bed chromatography using an Equilibrium-Dispersion Model: II. Experimental validation. *Chemical Engineering Science*, 226, 115808.

Lemoine-Nava, R. and Engell, S. (2014). Individual Column State and Parameter Estimation in the Simulated Moving Bed Process: an Optimization-based Method. *IFAC Proceedings Volumes*, 47(3), 9376–9381.

Mazzotti, M., Storti, G., and Morbidelli, M. (1997). Optimal operation of simulated moving bed units for nonlinear chromatographic separations. *Journal of Chromatography A*, 769(1), 3–24.

Rajendran, A., Paredes, G., and Mazzotti, M. (2009). Simulated moving bed chromatography for the separation of enantiomers. *Journal of Chromatography A*, 1216(4), 709–738.

Schmidt-Traub, H., Schulte, M., and Seidel-Morgenstern, A. (eds.) (2020). *Preparative Chromatography*. Wiley.

Toumi, A. and Engell, S. (2004). Optimization-based control of a reactive simulated moving bed process for glucose isomerization. *Chemical Engineering Science*, 59(18), 3777–3792.

von Lieres, E. and Andersson, J. (2010). A fast and accurate solver for the general rate model of column liquid chromatography. *Computers & Chemical Engineering*, 34(8), 1180–1191.